The Cryosphere, 6, 901–908, 2012
www.the-cryosphere.net/6/901/2012/
doi:10.5194/tc-6-901-2012

The Cryosphere

Ikaite crystals in melting sea ice – implications for pCO_2 and pH levels in Arctic surface waters

S. Rysgaard[1,2,3,6], R. N. Glud[3,4,5], K. Lennert[3], M. Cooper[2], N. Halden[1,2], R. J. G. Leakey[4], F. C. Hawthorne[2], and D. Barber[1]

[1]Centre for Earth Observation Science, CHR Faculty of Environment Earth and Resources, University of Manitoba, 499 Wallace Building, Winnipeg, MB R3T 2N2, Canada
[2]Department of Geological Sciences, CHR Faculty of Environment Earth and Resources, University of Manitoba, 499 Wallace Building, Winnipeg, MB R3T 2N2, Canada
[3]Greenland Climate Research Centre, Greenland Institute of Natural Resources, Kivioq 2, 3900 Nuuk, Greenland
[4]Scottish Association for Marine Science, Scottish Marine Institute, Oban. PA37 1QA, UK
[5]Southern Danish University and NordCEE, Odense M, Denmark
[6]Arctic Research Centre, Aarhus University, 8000 Aarhus C, Denmark

Correspondence to: S. Rysgaard (rysgaard@cc.umanitoba.ca)

Received: 18 February 2012 – Published in The Cryosphere Discuss.: 14 March 2012
Revised: 19 June 2012 – Accepted: 25 June 2012 – Published: 15 August 2012

Abstract. A major issue of Arctic marine science is to understand whether the Arctic Ocean is, or will be, a source or sink for air–sea CO_2 exchange. This has been complicated by the recent discoveries of ikaite (a polymorph of $CaCO_3 \cdot 6H_2O$) in Arctic and Antarctic sea ice, which indicate that multiple chemical transformations occur in sea ice with a possible effect on CO_2 and pH conditions in surface waters. Here, we report on biogeochemical conditions, microscopic examinations and x-ray diffraction analysis of single crystals from a melting 1.7 km^2 (0.5–1 m thick) drifting ice floe in the Fram Strait during summer. Our findings show that ikaite crystals are present throughout the sea ice but with larger crystals appearing in the upper ice layers. Ikaite crystals placed at elevated temperatures disintegrated into smaller crystallites and dissolved. During our field campaign in late June, melt reduced the ice floe thickness by 0.2 m per week and resulted in an estimated 3.8 ppm decrease of pCO_2 in the ocean surface mixed layer. This corresponds to an air–sea CO_2 uptake of 10.6 mmol m^{-2} sea ice d^{-1} or to 3.3 ton km^{-2} ice floe $week^{-1}$. This is markedly higher than the estimated primary production within the ice floe of 0.3–1.3 mmol m^{-2} sea ice d^{-1}. Finally, the presence of ikaite in sea ice and the dissolution of the mineral during melting of the sea ice and mixing of the melt water into the surface oceanic mixed layer accounted for half of the estimated pCO_2 uptake.

1 Introduction

Recent work suggests that sea ice may play a central role in the control of the air–sea CO_2 flux in high latitude areas (Rysgaard et al., 2011; Loose and Schlosser, 2011; Geilfus et al., 2012). During winter, as sea ice grows, reduced air temperatures cause the brine volumes of surface sea ice to contract and permeability to decrease, effectively stopping air–sea ice gas exchange (Loose et al., 2011). At the same time brine volume contraction further increases brine salinity, CO_2 concentration, and supersaturation with respect to a suite of minerals, including several polymorphs of calcium carbonate ($CaCO_3$) (Assur, 1958). Crystallization of $CaCO_3$ [$Ca^{2+} + 2HCO_3^- \rightarrow CaCO_3(s) + H_2O + CO_2$] increases the concentration of CO_2 in the brine during growing sea ice conditions. Calcium carbonate crystals can be trapped in the ice matrix during brine rejection. This is equivalent to total alkalinity (TA) retention within the sea ice in the form of $CaCO_3$. In comparison, the total dissolved inorganic carbon (TCO_2) is more efficiently lost from the sea ice along with the rejected brine. This can lead to a higher $TA : TCO_2$ ratio in the sea ice brine upon $CaCO_3$ dissolution than the $TA : TCO_2$ ratio in the surface waters. This was observed recently in both Arctic and Antarctic sea ice (Rysgaard et al., 2007; Fransson et al., 2011). The observation of

TA : TCO_2 ratios as high as 2 indicate that calcium carbonate is formed in natural sea ice (Rysgaard et al., 2007, 2009). Ikaite crystals in sea ice have recently been discovered in both hemispheres (Dieckmann et al., 2008, 2010). The specific conditions promoting ikaite precipitation in sea ice are currently poorly understood, but if precipitation occurs in the porous bottom sea-ice layer, where the brine volume is larger than 5 % (Weeks and Ackley, 1986; Golden et al., 1998, 2007), the CO_2-enriched brine will exchange with seawater via gravity drainage (Notz and Worster, 2009). In contrast, the ikaite crystals could potentially remain trapped within the skeletal layer where they will act as a store of TA, which will become a source of excess TA to the ocean water upon subsequent mineral dissolution when sea ice melts during summer (Rysgaard et al., 2007, 2009, 2011; Nedashkovsky et al., 2009). This will lower the pCO_2 of surface waters affected by melting sea ice and cause an increase in the air–sea CO_2 flux. More knowledge is, however, needed in order to understand carbonate crystal distribution in sea ice and their fate during summer melt. Here, we report on biogeochemical conditions as well as microscopic examination and x-ray diffraction analysis of single ikaite crystals in a melting 1.7 km^2 drifting ice floe passing through the Fram Strait in late June 2010.

Fig. 1. Map of the study area. The northern "X" marks the studied sea ice floe position (81° N, 5° E) on 22 June and the southern "X" marks its position (80° N, 2° E) on the 30 June 2010.

2 Methods

The research was undertaken in summer 2010 as part of the ICE CHASER II research cruise on the UK icebreaker RRS *James Clark Ross* (JCR) (cruise JR219). The sampling location is presented in Fig. 1. On 22 June, the JCR was anchored to a 1.7 km^2 drifting ice floe at 81° N, 5° E and drifted with the floe to 80° N, 2° E on 30 June 2010. The JCR was used as a laboratory for processing samples collected on the ice floe. Sampling was performed about 0.5 km away from the ship and care was taken not to disturb the coring area that was reached from one side. Sea ice cores (9-cm diameter) were collected with a MARK II coring system (Kovacs Enterprises, USA) on three different sampling dates. We recognize that brine may have been lost upon extraction of the core from the ice (Barber and Yackel, 1999). We estimate brine loss to be approximately 10 percent (±5 %) based on unpublished data collected during the IPY-CFL project in 2008. The measurements were done by replicate samplings (core extraction) from a small area of uniform first-year sea ice (area of about 10 m^2). Salinity was measured from these cores, and the variability in the measurements was used to estimate the potential brine loss. Thus, the expectation was that the brine volumes would be approximately equal over this small area, and most of the variability would be due to variable brine drainage. However, brine loss from handling the ice core sections in the laboratory (see below) was minor, as evaluated from the few droplets left in the polyethylene jars and on the clean sheets on which we worked. On each occasion, snow and sea ice thickness were recorded. Vertical temperature profiles were measured with a thermometer (Testo, Lenzkirch, Germany, and accuracy 0.1 °C) at 10-cm intervals in the snow and at the center of the cores through 3-mm holes drilled immediately after coring. Each sea ice core (one every sampling date) was then cut into 10-cm sections, and each section was transferred to a 1-liter polyethylene jar and kept cold (insulated thermo box) until further processing within an hour in the JCR laboratories. Water samples from 1 m below the sea ice were collected for salinity, temperature, TA and TCO_2 determinations with a glass syringe fitted with a gas tight Tygon tube inserted through the ice.

In the laboratory, sea ice density was determined by shaping the ice core section into well defined pieces with planar sides and then measuring the volume and weight of each piece. The pieces were then cut in two. One half was melted within 2 h, and 25 ml was collected for salinity measurements. The salinity of the melted sections (bulk salinity) was determined with a sonde (Knick Konduktometer, Germany) calibrated to a PORTASAL salinometer. Brine volume in sea ice was calculated according to Cox and Weeks (1983) for temperatures below −2 °C, and according to Leppäranta and Manninen (1988) for temperatures within the range 0 °C to −2 °C. The rest of the meltwater was filtered through a GF/F filter for determination of chlorophyll *a* (Chl *a*) concentration. Chl *a* was extracted from filters for 24 h in 95 % buffered acetone and analyzed by high performance liquid chromatography (HPLC) (Mantoura et al., 1997).

The other half of each sea ice section was used to determine TA and TCO_2 concentrations in the following way: The ice segment was placed immediately in a gas-tight laminated (Nylon, ethylene vinyl alcohol, and polyethylene) plastic bag (Hansen et al., 2000) fitted with a 50-cm gas-tight Tygon tube and a valve for sampling. The weight of the

bag containing the sea ice sample was recorded. Cold (1 °C) deionized water (25–50 ml) of known weight and TA and TCO_2 concentrations was added together with 50 µl $HgCl_2$ (saturated solution). The plastic bag was then closed immediately, and excess air and as much deionized water as possible quickly removed through the valve; then the plastic bag was weighed again. The weight of the deionized water accounted for 8–15 % of the sea ice weight. The sea ice was melted in the deionized water (at 0 °C), and the meltwater mixture transferred to a gas-tight vial (12 ml Exetainer, Labco High Wycombe, UK). Deionized water was added in order to remove all the excess air, and as much deionized water as possible was quickly removed through the valve; the plastic bag was then weighed again. The melt water mixture and bubbles released from the melting sea ice were transferred to gas-tight vials. In order to minimize gas exchange between brine and the ambient atmosphere, handling of each sea ice section took few minutes and a sea ice core could be processed within half an hour. Any $CaCO_3$ crystals present in the ice core sections used for this analysis were expected to have dissolved during sampling processing, contributing to the measured TA and TCO_2 concentrations. Standard methods of analysis were used: TCO_2 concentrations were measured on a coulometer (Johnson et al., 1987), TA by potentiometric titration (Haraldsson et al., 1997), and gaseous CO_2 by gas chromatography. Routine analysis of Certified Reference Materials (provided by A. G. Dickson, Scripps Institution of Oceanography) verified that TCO_2 and TA concentrations ($n = 3$) could be analyzed within ± 1 µmol kg^{-1} and ± 4 µmol kg^{-1}, respectively. Bulk concentrations of TA and TCO_2 in the sea ice (C_i) were calculated as:

$$C_i = \frac{C_m W_m - C_a W_a}{W_i} \quad (1)$$

where C_m is the TA or TCO_2 concentration in the meltwater mixture, W_m the weight of the meltwater mixture, C_a the TA or TCO_2 concentration in the deionized water, W_a the weight of the deionized water, and W_i the weight of the sea ice.

Following the determination of TCO_2 and TA, the bulk partial pressure of CO_2 (pCO_2) and pH (on the total scale) were computed using the temperature and salinity conditions in the field and a standard set of carbonate system equations, excluding nutrients, with the CO2SYS program of Lewis and Wallace (2012). We used the equilibrium constants of Mehrbach et al. (1973) refitted by Dickson and Millero (1987, 1989).

On 29 June, a sea ice core was collected for visualization and identification of $CaCO_3$ crystals in sea ice. The sea ice core was cut into 10-cm sections and transferred to 1-liter polyethylene jars. The jars were transferred to a temperature controlled laboratory on board the JCR, and each 10-cm section of sea ice was cut into small pieces with a stainless steel knife and allowed to melt slowly over 12 h at −0.2 °C. The jars were then carefully swirled so crystals would concentrate at the bottom center of the jar. A portion of the crystals was then pipetted into a plankton counting chamber for microscopic examination at 100 and 200 magnification using a Zeiss (Carl Zeiss, Welwyn Garden City, UK) Axiovert S100 inverted microscope fitted with an AxioCam HRc digital camera and AvioVision version 4.7 image analysis software. Ten to fifteen images of crystals were obtained from each section. Using the microscope, we soon realized that it was possible to observe ikaite crystals dissolve when temperature was allowed to increase above 4 °C. Therefore, a dissolution experiment was performed on single crystals collected from the uppermost 0–10 cm section. Images of the crystals were obtained 80 times over 400 min while temperature was allowed to increase above 4 °C. The potential for loss of brine upon extraction from the sea ice may have affected both rates and magnitudes of processes reported. We expected that, in general, our estimates would be proportionally underestimated due to the brine loss. Sections of a parallel sea ice core (entire core) were kept at −18 °C and brought to the x-ray laboratory at the Department of Geological Sciences at the University of Manitoba. There, sea ice was melted as described above, and a small droplet of cold water containing transparent crystals was deposited onto a cold glass slide resting on a chilled aluminum block containing a 1-cm central viewing hole. The crystals were first examined with a polarized light microscope to assess their optical properties and then mounted for x-ray study using a stereo binocular microscope. Selected crystals from 0–10 cm, 10–20 cm, and 40–50 cm sections (distance from top of the sea ice) were dragged across the cold glass slide from the water droplet using a metal probe, and immersed into a drop of special purpose sampling oil, which restricted sublimation. Each crystal was then scooped up with a low x-ray scattering micro-loop and rapidly transferred to the nitrogen cold stream (−20 °C) on the x-ray diffraction instrument with a magnetic coupling goniometer head. The x-ray diffraction instrument consisted of a Bruker D8 three-circle diffractometer equipped with a rotating anode generator (Mo$K\alpha$ X-radiation), multi-layer optics, APEX-II CCD detector, and an Oxford 700 Series liquid-N Cryostream. The intensities of more than 100 reflections were harvested from six frame series (each spanning 15° in either ω or ϕ) collected to 60° 2θ using 0.6 s per 1° frame with a crystal-to-detector distance of 5 cm. In total, 14 crystals were identified through successful indexing of observed x-ray diffraction maxima onto known characteristic unit cells. Of these, 4 were ikaite and exhibited a distinct morphology, as compared to other crystals identified as feldspar, quartz and corundum. After the discovery onboard JCR that ikaite crystals had a distinct morphology (rhombs, thinner plates) and that they dissolved at elevated temperature, or by adding acid, the dimensions of 127 ikaite crystals, identified by light microscopy, were measured, and the crystals grouped into size categories for describing the vertical size distribution through the ice. The procedure was to take a photo of a cold sample, then warm it up for 5–10 min and take a photo again. Crystals dissolving were assumed

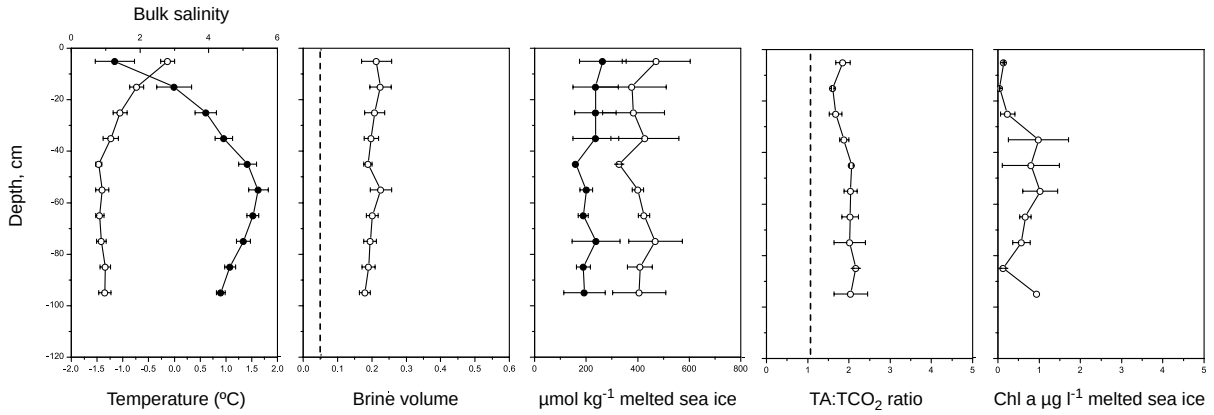

Fig. 2. Average conditions of temperature (open circles), bulk salinity (closed circles), brine volumes, TA (open circles), TCO_2 (closed circles), TA : TCO_2 ratio and Chl *a* at the coring site of the sea ice floe sampled during 22 to 30 June 2010. Values for temperature, salinity and brine volume are mean ± standard deviation ($n = 10$) and for TA, TCO_2, and Chl *a* ($n = 3$).

to be ikaite. After melting the samples at room temperature for 24 h, all ikaite crystals disappeared and crystals left behind were analyzed on x-ray. They were feldspar and quartz, and a single crystal of corundum. Morphologically, they differed from ikaite by not being crystal clear, having a different shape, and with color. The number of ikaite crystals was very high and by far exceeded any other crystals in the sea ice.

In summary, bulk sea ice temperature, salinity, and brine volume were derived from 10 ice cores; TA, TCO_2 and Chl *a* were obtained from 3 ice cores; and ikaite crystal microscopy and distribution with depth in the ice were conducted on 1 core on 29 June. Mineral phase identification by x-ray diffraction was performed on material extracted from reserved core stored at −18 °C.

3 Results

The average sea ice thickness at the sampling site, as determined from coring, decreased from 100 (±5) cm to 80 (±6) cm from 22 June to 29 June (2–3 cm d^{-1}) while the ice floe was drifting SSW. The decayed ice surface of 1–2 cm thickness on 22 June reduced to a mm thick layer during the 8 day sampling period. Air temperatures and water column temperatures 20 cm beneath the sea ice fluctuated around 0 °C (Table 1). Sea ice temperatures varied from 0 to −1.7 °C, indicating a rapidly melting ice floe (Fig. 2).

Bulk salinity over the study period varied from 0.2 to 6. The high temperatures and low salinities caused brine volume to be high. Average brine volumes during 22, 25 and 29 June were 0.16, 0.21 and 0.19, respectively. Brine volumes > 0.05 indicated that the sea ice was very permeable (Freitag and Eicken, 2003). A slight increase in the average TCO_2 and TA conditions was observed over the sampling period (Table 2). Concentrations of TCO_2 and TA in the vertical profiles (including dissolved ikaite) varied from 80

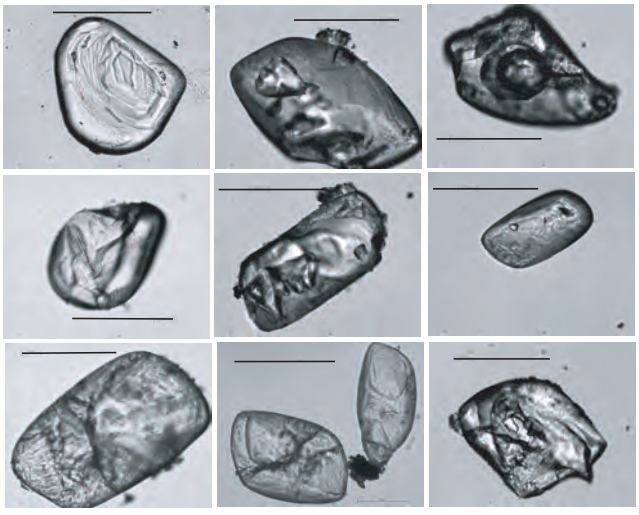

Fig. 3. Examples of ikaite crystals found in the sea ice. Scale bar is 100 µm.

to 435 µmol kg^{-1} melted sea ice and 210 to 680 µmol kg^{-1} melted sea ice, respectively. The TA : TCO_2 ratio in sea ice was on all sampling dates significantly higher than in the water column (Tables 1, 2). Chlorophyll *a* values in the sea ice ranged from 0.03 to 2.4 µg kg^{-1} melted sea ice with highest concentration in the central part of the sea ice.

The crystals (10 to 1000 µm in size) observed in the sea ice were highly transparent with a rounded rhombic morphology (Fig. 3) and showed uniform extinction under cross-polarized light, suggesting that they were simple single crystals. All reflections fitted well to a monoclinic C-centered cell with (a) = 8.806(2), (b) = 8.315(2), (c) = 11.027(2), Å $\beta = 110.571(12)$, and $V = 755.9(4)$. From the general appearance, optical properties and unit-cell determination, the crystals examined were ikaite (Hesse and Küppers, 1983). The

Table 1. Surface water conditions (20 cm below sea ice) of temperature, salinity, TCO_2, TA and pCO_2 during the field campaign. Data from triplicate samples collected on three separate occasions are shown.

Date 2010	TCO_2 µmol kg^{-1}	TA µmol kg^{-1}	TA : TCO_2	T (°C)	Salinity	pH	pCO_2 µatm
25 June	1968.9	2201.5	1.12	−0.08	32.64	8.36	163
	1965.0	2196.9	1.12	−0.09	32.62	8.36	163
	1985.8	2197.6	1.11	−0.07	32.56	8.31	183
27 June	2005.9	2252.7	1.12	−0.49	33.27	8.38	157
	2010.8	2235.8	1.11	−0.04	32.59	8.33	176
	2016.2	2243.5	1.11	−0.70	32.64	8.35	169
29 June	1982.4	2173.2	1.10	−0.01	32.19	8.27	202
	1984.8	2168.9	1.09	−0.06	32.31	8.26	210
	1967.2	2160.8	1.10	−0.09	32.33	8.28	197

Table 2. Sea ice meltwater conditions of temperature, salinity, TCO_2, TA and pCO_2 during the field campaign. Values are mean ± standard deviation ($n = 10$) of vertical profile data from sea ice cores collected on the respective dates with pCO_2 conditions calculated at 0 dbar and 0 °C.

Date 2010	TCO_2 µmol kg^{-1}	TA µmol kg^{-1}	TA: TCO_2	T (°C)	Salinity	pH (at 0 °C)	pCO_2 µatm (at 0 °C)
25 June	142.3 ± 23.9	304.4 ± 62.6	2.1	−1.3 ± 0.4	3.8 ± 1.3	10.1 ± 0.2	0.2 ± 0.1
27 June	229.0 ± 98.8	421.3 ± 126.1	1.8	−1.0 ± 0.5	4.2 ± 1.8	9.9 ± 0.3	0.5 ± 0.4
29 June	291.5 ± 116.5	533.0 ± 137.3	1.8	−1.1 ± 0.5	3.8 ± 1.8	10.1 ± 0.4	0.3 ± 0.5

crystals identified as ikaite have a very distinct morphology, and are easily recognized – the only significant variation we saw was a thinner plate morphology in addition to the more common thicker rhombs. Ikaite crystals were distributed throughout the sea ice with higher proportion of larger (> 100 µm size) crystals in the surface layers of the ice (Fig. 4). A crystal of ikaite, identified by single crystal x-ray diffraction, was allowed to decompose by raising the temperature above 4 °C over 4 h (Fig. 5). This crystal lost its transparency and gradually disaggregated into a multitude of smaller crystal components that resembled ikaite under the optical microscope. Of these, one tiny (∼ 20 µm) fragment was harvested and examined by x-ray diffraction, and was found to be ikaite as well. We have experimental evidence, from the Sea ice Environmental Research Facility (SERF) mesocosm located at the University of Manitoba (Canada) and from a recent winter field campaign to Northeastern Greenland, that ikaite crystals form within hours in new ice but also form in the interior of thicker ice (data to be presented elsewhere). In contrast, the crystals of quartz, feldspar, and corundum also observed inside the sea ice matrix must have been entrained during ice formation.

4 Discussion

The sea ice floe melted rapidly during the investigation period as it drifted SSW in the Fram Strait. This was evident from the ca. 20 cm week^{-1} decrease in thickness, the reduction of bulk salinity, and the very high brine volumes in the entire sea ice column. Much lower TA and TCO_2 concentrations in sea ice were measured as compared to the underlying water (Tables 1, 2). The TCO_2 concentration in the sea ice was ca. 10 % of the TCO_2 concentration in the underlying water, and TA concentration in sea ice was ca. 20 % of the TA in the water below. This, together with the higher TA : TCO_2 ratio of 1.83 to 2.12 in the sea ice as compared with the underlying water (1.09 to 1.12), is in line with formation of carbonate crystals within the sea ice. Assuming that sea ice is formed from surface water with a TA : TCO_2 ratio of 1, the TA : TCO_2 ratio of 1.83 to 2.12 observed in the sea ice could be generated by a carbonate crystal concentration of 162.1 to 241.5 µmol kg^{-1} melted sea ice. This is high compared with estimates from Antarctica (Dieckmann et al., 2008). Ikaite concentrations in our study are 1.5 to 2.2 times higher than the highest concentration reported from Antarctica. On areal basis the ikaite concentration is more than 10 fold higher. Chl *a* and a diverse microbial community were also observed within the sea ice in several of our ice cores, supporting previous findings of internal sea ice algal communities (Mock and Gradinger, 1999).

Various ikaite crystals were isolated from the sea ice (Fig. 3). These ranged in size from 10 µm to large mm-size crystals. They were all highly transparent with a rounded rhombic morphology and showed uniform extinction under crossed polarized light, suggesting that they were all well-crystallined simple single crystals. The crystals identified by

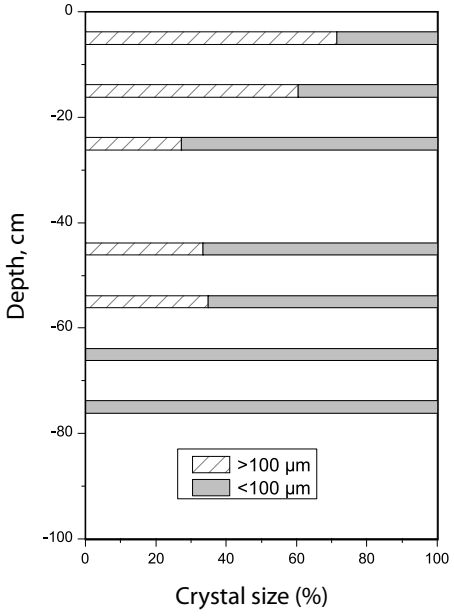

Fig. 4. Vertical distribution of small (< 100 µm) and large (> 100 µm) ikaite crystals in the sea ice.

x-ray diffraction as ikaite had a morphology similar to the ones reported from Antarctica (Dieckmann et al., 2008) and from Arctic coastal fast ice locations in Svalbard (Dieckmann et al., 2010) and off Station Nord NE Greenland (Rysgaard et al., unpublished results). Furthermore, we observed ikaite crystals throughout the sea ice column with the largest crystals in the upper layers of the sea ice, in agreement with the observations from the other locations. Our ikaite data originating from the offshore Fram Strait thus strongly suggest that ikaite crystals within the sea ice matrix are representative for ice of the Arctic basin.

Ikaite crystals are considered stable at temperatures below 4 °C. At room temperature ikaite is unstable and decomposes into anhydrous calcium carbonate, vaterite and/or calcite and water (Marland, 1975; Shaikh, 1990; Mikkelsen et al., 1999). Furthermore, relative humidity has been identified as an important factor controlling the rate of decomposition of ikaite (Mikkelsen et al., 1999). The observation that a crystal of ikaite, identified by single crystal x-ray diffraction, disintegrated into smaller crystallites and eventually dissolved when temperatures increased above 4 °C over a few hours (Fig. 5) confirms that ikaite crystals are highly unstable. Dissolving could in principle also be related to ikaite's reaction with CO_2 in the atmosphere or from interaction with the carbonate system in the water column changing the pH of the ikaite crystals' surroundings. More work is needed to resolve the kinetics of dissolving ikaite crystals in sea ice. Melting of sea ice sections in gas tight bags at 0 °C also resulted in very low CO_2 levels in bulk sea ice sections throughout the ice column (Table 2). In addition, pH values increased to 10 in

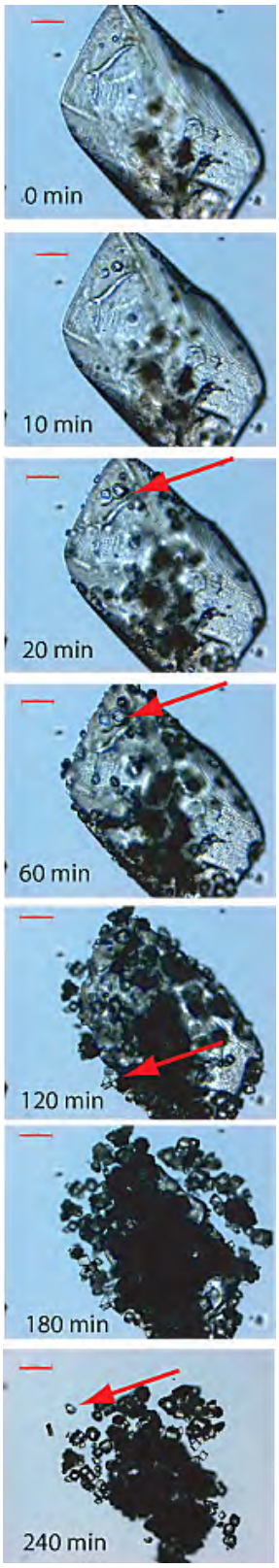

Fig. 5. Ikaite crystal dissolution during melting of sea ice over 240 min. Arrows point at smaller sub-units of crystals (also ikaite) that emerge during melting. Scale bar is 50 µm.

the bulk sections. It is likely that ikaite crystals in the lower parts of the sea ice will disintegrate before the ikaite crystals higher up in the sea ice, as they will be in closer contact with the carbonate system of the underlying water due to higher brine volumes in these lower ice layers earlier in the melting season. This would explain why the largest crystals remained in the upper ice layers (Fig. 4). Another explanation for the largest ikaite crystals being found in the top layers of the sea ice is because they had the greatest opportunity (i.e. time) to grow into bigger crystals.

Melting of sea ice and dissolution of ikaite crystals will affect pCO_2 levels and the pH of surface water. We observed pCO_2 levels within sea ice of < 1 µatm, and melting sea ice contributed to the low pCO_2 conditions in surface waters (157–210 µatm) as compared with the 387 µatm in the atmosphere (Tables 1, 2). In addition, pH in melting sea ice was high (pH = 9.9–10.1) and affected pH of surface waters (pH = 8.3–8.4). Assuming that all ikaite crystals dissolve in the sea ice or in the mixed layer, melting of 0.2 m sea ice – with average temperature (−1.1 °C), salinity (3.9), TA (420 µmol kg^{-1}) and TCO_2 (221 µmol kg^{-1}) from Table 2 – into a 20-m thick mixed layer – with average water column characteristics of temperature (−0.2 °C), salinity (32.6), TA (2203 µmol kg^{-1}) and TCO_2 (1987 µmol kg^{-1}) from Table 1 – will result in a 3.8 ppm decrease in pCO_2 per week. This decrease is calculated from the resultant conditions in a 20-m mixed layer – temperature (−0.2 °C), salinity (32.2), TA (2186 µmol kg^{-1}) and TCO_2 (1970 µmol kg^{-1}) – using the CO2SYS program (see materials and methods). Assuming no $CaCO_3$ crystals, e.g. TA and TCO_2 concentrations are both 221 µmol kg^{-1}, the resultant pCO_2 decrease will be 2.2 ppm per week. Based on average conditions during the field campaign (Tables 1 and 2), this corresponds to an air–sea CO_2 uptake of 10.6 mmol m^{-2} sea ice d^{-1}, or to 3.3 ton CO_2 km^{-2} ice floe week^{-1} (with $CaCO_3$) and 4.9 mmol m^{-2} sea ice d^{-1}, or 1.5 ton CO_2 km^{-2} ice floe week^{-1} (without $CaCO_3$). It should be noted that we do not take wind mixing into account, but just consider the resultant CO_2 uptake of melting 0.2 m sea ice into a 20-m mixed layer after a return to initial pCO_2 conditions. An important finding here is that presence of $CaCO_3$ in sea ice will double the air–sea flux as compared to melting of pure sea ice. This sea ice driven CO_2 uptake is higher than the estimated primary production within the ice floe of 0.3–1.3 mmol m^{-2} sea ice d^{-1} (Glud et al., work in progress), as assessed from > 100 measurements of primary production incubations using ^{14}C. Thus, sea ice melting plays a more important role in atmospheric CO_2 uptake than concurrent primary productivity of sea ice algae. This role is further enhanced by the dissolution of the authigenic $CaCO_3$ content of the sea ice in the form of ikaite.

In the present study we melted sea ice at 0 °C to isolate ikaite crystals. However, we do not know if other carbonate crystals were present in the sea ice and dissolved by our melting procedure. Nor do we know if ikaite crystal continuously form and dissolve during the season; a process, which could greatly increase the air–sea CO_2 flux. A conceptual model on the processes driving air–sea gas exchange throughout the cycle of sea ice formation and decay was recently provided by Rysgaard et al. (2011). It was suggested that ice growth during winter results in the rejection of CO_2 along with salts dissolved in seawater from the ice crystal matrix, which gives rise to dense brine that sinks and is incorporated into intermediate and deep water layers. Subsequent sea ice melt leads to stratification of the surface water column and mixing with melt water already low in TCO_2 from biological uptake and from excess TA from the internal sea ice $CaCO_3$ cycle. The net result will be an increase in TA and a lowering of CO_2 in the stratified surface waters, enhancing the air–sea CO_2 flux. Our present study performed in and below an actively melting ice floe supports the conceptual model and provides evidence that melting sea ice and the dissolution of its authigenic $CaCO_3$ content indeed lead to an increased CO_2 flux from the atmosphere to the ocean. In addition, dissolving carbonate crystals will increase pH in surface waters exposed to melting sea ice.

5 Conclusions

Our study shows that ikaite crystals were present throughout the ice column of a drifting sea ice floe in the Fram Strait. Larger crystals were observed in surface layers. Melting of the sea ice caused extremely low pCO_2 conditions within sea ice (< 1 µatm) and contributed to the low pCO_2 conditions in surface waters (157–210 µatm). In addition, pH in melting sea ice was high (pH = 9.9–10.1) and affected pH of surface waters (pH = 8.3–8.4). Melting of sea ice and the dissolution of its authigenic ikaite content during June was estimated to be responsible for an air–sea CO_2 uptake of 10.6 mmol m^{-2} sea ice d^{-1}. This is higher than the estimated primary production within the ice floe of 0.3–1.3 mmol m^{-2} sea ice d^{-1}. Finally, dissolution of ikaite crystals doubled the air–sea CO_2 uptake as compared with melting of ikaite-free sea ice.

Acknowledgements. The study received financial support from the Danish Agency for Science, Technology and Innovation, the Canada Excellence Research Chair (CERC) program, and the UK Natural Environmental Research Council Oceans 2025 strategic marine research programme. The study is a part of the Greenland Climate Research Center's activities, GCRC6507 (www.natur.gl). We are grateful to the captain, officers and crew of the RSS *James Clark Ross* for their assistance during the study and to Anna Haxen, Louise Mølgaard, Thomas Krogh, Debra Brennan, Sian Lordsmith and Tim Brand for technical assistance in the laboratory.

Edited by: H. Eicken

References

Assur, A.: Composition of sea ice and its tensile strength, in Arctic Sea Ice, Natl. Res. Counc. Publ. Natl. Acad. Sci. Natl. Res. Counc., Washington DC, 598, 106–138, 1958.

Barber, D. G. and Yackel, J.: The physical, radiative and microwave scattering characteristics of melt ponds on sea ice, Int. J. Remote Sensing, 20, 2069–2090, 1999.

Cox, G. F. N. and Weeks, W. F.: Equations for determining the gas and brine volumes in sea ice samples, J. Glaciol., 29, 306–316, 1983.

Dickson, A. G. and Millero, F. J.: A comparison of the equilibrium constants for the dissociation of carbonic acid in seawater media, Deep-Sea Res., 34, 1733–1743, 1987.

Dickson, A. G. and Millero, F. J.: Corrigenda, Deep-Sea Res., 36, 983, 1989.

Dieckmann, G. S., Nehrke, G., Papadimitriou, S., Göttlicher, J., Steininger, R., Kennedy, H., Wolf-Gladrow, D., and Thomas, S. N.: Calcium carbonate as ikaite crystals in Antarctic sea ice, Geophys. Res. Lett., 35, L08501, doi:10.1029/2008GL033540, 2008.

Dieckmann, G. S., Nehrke, G., Uhlig, C., Göttlicher, J., Gerland, S., Granskog, M. A., and Thomas, D. N.: Brief Communication: Ikaite (CaCO3·6H2O) discovered in Arctic sea ice, The Cryosphere, 4, 227–230, doi:10.5194/tc-4-227-2010, 2010.

Fransson, A., Chierici, M., Yager, P. L., and Smith Jr., W. O.: Antarctic sea ice carbon dioxide system and controls, J. Geophys. Res., 116, C12035, doi:10.1029/2010JC006844, 2011.

Freitag, J. and Eicken, H.: Meltwater circulation and permeability of Arctic summer sea ice derived from hydrological field experiments, J. Glaciol., 49, 349–358, 2003.

Geilfus, N.-X., Carnat, G., Papakyriakou, T., Tison, J.-L., Else, B., Thomas, H., Shadwick, E., and Delille, B.: Dynamics of pCO_2 and related air-ice CO_2 fluxes in the Arctic coastal zone (Amundsen Gulf, Beaufort Sea), J. Geophys. Res., 117, C00G10, doi:10.1029/2011JC007118, 2012.

Golden, K. M., Eicken, H., Heaton, A. L., Miner, J., Pringle, D. J., and Zhu, J.: Thermal evolution of permeability and microstructure in sea ice, Geophys. Res. Lett. 34, L16501, doi:10.1029/2007GL030447, 2007.

Golden, K. M., Ackley, S. F., and Lytle, V. I.: The percolation phase transition in sea ice, Science, 282, 2238–2241, 1998.

Hansen, J. W., Thamdrup, B., and Jørgensen, B. B.: Anoxic incubation of sediment in gas tight plastic bags: A method for biogeochemical process studies, Mar. Ecol. Prog. Ser., 208, 273–282, 2000.

Haraldsson, C., Anderson, L. G., Hasselöv, M., Hult, S., and Olsson, K.: Rapid, high-precision potentiometric titration of alkalinity in ocean and sediment pore water, Deep-Sea Res. Pt. I, 44, 2031–2044, 1997.

Hesse, K. F. and Küppers, H.: Refinement of the structure of Ikaite, $CaCO_3{\cdot}6H_2O$, Zeitschrift für Krystallographie 163, 227–231, 1983.

Johnson, K. M., Sieburth, J. M., Williams, P. J., and Brändström, L.: Coulometric total carbon dioxide analysis for marine studies: Automation and calibration, Mar. Chem., 21, 117–133, 1987.

Leppäranta, M. and Manninen, T.: The brine and gas content of sea ice with attention to low salinities and high temperatures, Finnish Institute of Marine Research Internal Report, Helsinki, Finland, 1988, 15 pp., 1988.

Lewis, E. and Wallace D.: The program CO2SYS.EXE can be downloaded at: http://cdiac.esd.ornl.gov/oceans/co2rprtnbk.html, 2012.

Loose, B. and Schlosser P.: Sea ice and its effect on CO_2 flux between the atmosphere and the Southern Ocean interior, J. Geophys. Res., 116, C11019, doi:10.1029/2010JC006509, 2011.

Loose, B., Schlosser, P., Perovich, P., Ringelberg, D., Ho, D. T., Takahashi, T., Richter-Menge, J., Reynolds, C. M., McGillis, W. R., and Tison, J.-L.: Gas diffusion through columnar laboratory sea ice: implications for mixed-layer ventilation of CO_2 in the seasonal ice zone, Tellus, 63B, 23–39, 2011.

Mantoura, R. F. C., Barlow, R. G., and Head, E. J. H.: Simple isocratic HPLC methods for chlorophylls and their degradation products, in: Phytoplankton pigments in oceanography: guidelines to modern methods, edited by: Jeffrey, S. W., Mantoura, R. F. C., and Wright, S. W., UNESCO, Paris, 307–326, 1997.

Marland, G.: The stability of $CaCO_3.6H_2O$ (ikaite), Geochim. Cosmochim. Acta, 39, 83–91, 1975.

Mehrbach, C., Culberson, H., Hawley, J. E., and Pytkowicz, R. M.: Measurement of the apparent dissociation constants of carbonic acid in seawater at atmospheric pressure, Limnol. Oceanogr., 18, 897–907, 1973.

Mikkelsen, A., Andersen, A. B., Engelsen, S. B., Hansen, H. C., Larsen, O., and Skibsted, L. H.: Presence and dehydration of ikaite, calcium carbonate hexahydrate, in frozen shrimp shell, J. Agric. Food Chem., 47, 911–917, 1999.

Mock, T. and Gradinger, R.: Determination of Arctic ice algal production with a new in situ incubation technique, Mar. Ecol. Prog. Ser., 177, 15–26, 1999.

Nedashkovsky, A. P., Khvedynich, S. V., and Petovsky, T. V.: Alkalinity of sea ice in the high-latitudinal arctic according to the surveys performed at north pole drifting station 34 and characterization of the role of the arctic in the CO_2 exchange, Oceanology, 49, 55–63, doi:10.1134/s000143700901007x, 2009.

Notz, D. and Worster, M. G.: Desalination processes of sea ice revisited, J. Geophys. Res., 114, C05006, doi:10.1029/2008JC004885, 2009.

Rysgaard, S., Glud, R. N., Sejr, M. K., Bendtsen, J., and Christensen, P. B.: Inorganic carbon transport during sea ice growth and decay: A carbon pump in polar seas, J. Geophys. Res., 112, C03016, doi:10.1029/2006jc003572, 2007.

Rysgaard, S., Bendtsen, J. B., Pedersen, L. T., Ramløv, H., and Glud, R. N.: Increased CO_2 uptake due to sea-ice growth and decay in the Nordic Seas, J. Geophys. Res., 114, C09011, doi:10.1029/2008JC005088, 2009.

Rysgaard, S., Bendtsen, J., Delille, B., Dieckmann, G., Glud, R. N., Kennedy, H., Mortensen, J., Papadimitriou, S., Thomas, D., and Tison, J.-L.: Sea ice contribution to air-sea CO_2 exchange in the Arctic and Southern Oceans, Tellus B, 63, 823–830, doi:10.1111/j.1600-0889.2011.00571.x, 2011.

Shaikh, A. M.: A new crystal growth form of vaterite, $CaCO_3$, J. Appl. Cryst., 23, 263–265, 1990.

Weeks, W. F. and Ackley, S. F.: The growth, structure and properties of sea ice, in: The Geophysics of Sea Ice, edited by: Untersteiner, N., Plenum, New York, 1986.